Functional Integration of Dopaminergic Neurons Directly Converted from Mouse Fibroblasts

Cell Stem Cell
Brief Report

Functional Integration of Dopaminergic Neurons Directly Converted from Mouse Fibroblasts

Jongpil Kim,[1] Susan C. Su,[3,4] Haoyi Wang,[1] Albert W. Cheng,[1,2] John P. Cassady,[1,2] Michael A. Lodato,[1,2] Christopher J. Lengner,[1] Chee-Yeun Chung,[1] Meelad M. Dawlaty,[1] Li-Huei Tsai,[3,4] and Rudolf Jaenisch[1,2,*]
[1]Whitehead Institute for Biomedical Research
[2]Department of Biology
Massachusetts Institute of Technology, Cambridge, MA 02142, USA
[3]Department of Brain and Cognitive Sciences, Picower Institute for Learning and Memory, Massachusetts Institute of Technology, Cambridge, MA 02139, USA
[4]Howard Hughes Medical Institute
*Correspondence: jaenisch@wi.mit.edu
DOI 10.1016/j.stem.2011.09.011

SUMMARY

Recent advances in somatic cell reprogramming have highlighted the plasticity of the somatic epigenome, particularly through demonstrations of direct lineage reprogramming of one somatic cell type to another by defined factors. However, it is not clear to what extent this type of reprogramming is able to generate fully functional differentiated cells. In addition, the activity of the reprogrammed cells in cell transplantation assays, such as those envisaged for cell-based therapy of Parkinson's disease (PD), remains to be determined. Here we show that ectopic expression of defined transcription factors in mouse tail tip fibroblasts is sufficient to induce Pitx3+ neurons that closely resemble midbrain dopaminergic (DA) neurons. In addition, transplantation of these induced DA (iDA) neurons alleviates symptoms in a mouse model of PD. Thus, iDA neurons generated from abundant somatic fibroblasts by direct lineage reprogramming hold promise for modeling neurodegenerative disease and for cell-based therapies of PD.

Parkinson's disease (PD) is one of the most common neurodegenerative disorders and is characterized by a loss of dopaminergic (DA) neurons, primarily of the substantia nigra pars compacta (SN), leading to a reduction of dopamine in the striatum (Berke and Hyman, 2000; Huse et al., 2005). While several possible cell sources, including fetal brain cells, ESCs, and iPSCs, are being explored as cell replacement therapies for degenerating DA neurons, ethical and practical barriers to the application of such therapies exist (Kim et al., 2002; Olanow et al., 1996; Wernig et al., 2008). Epigenetic reprogramming to pluripotency has provided critical evidence for the plasticity of the somatic genome (Eggan et al., 2004; Wilmut et al., 1997), and recent studies have demonstrated the feasibility of direct lineage reprogramming from one somatic cell type to another, bypassing a pluripotent intermediate state (Ieda et al., 2010; Szabo et al., 2010; Vierbuchen et al., 2010; Zhou et al., 2008). Two recent studies reported the generation of DA neurons by direct reprogramming (Caiazzo et al., 2011; Pfisterer et al., 2011). However, in these studies the gene expression profiles of reprogrammed DA neurons differed significantly from primary midbrain DA neurons. Furthermore, induced DA (iDA) neurons were not shown to be functional by in vivo transplantation assays. Thus, to assess the therapeutic potential of lineage-converted cells, we examined whether alternative induction strategies could generate iDA neurons that resemble midbrain DA neurons more closely and are functional in transplantation assays.

To analyze fibroblast reprogramming to DA neurons, we generated a knockin (KI) mouse model in which the *eGFP* coding sequence was targeted to the *Pitx3* gene under control of the endogenous promoter (Pitx3-eGFP) (Figures S1A and S1B available online). Previously, GFP+ cells derived from Pitx3-eGFP KI ESCs and mice have been shown to be functional midbrain DA neurons and to effectively alleviate symptoms in PD animal models (Hedlund et al., 2008; Zhao et al., 2004), while other reporter systems such as tyrosine hydroxylase (TH)-GFP were less effective (Hedlund et al., 2007). eGFP expression in DA neurons was assessed after in vitro differentiation of Pitx3-eGFP ESCs, and adult mice generated from Pitx3-eGFP ESCs exhibited eGFP+ DA neurons in the midbrain that were also positive for TH, a marker of mature DA neurons (Figures S1C and S1D). These data show that the Pitx3-eGFP KI model faithfully induced eGFP expression in midbrain DA neurons, thus providing a useful system for the isolation of iDA neurons.

To exclude the possibility of progenitor cell contamination in preparations of embryonic fibroblasts, we prepared tail tip fibroblasts (TTFs) from adult Pitx3-eGFP mice, which were GFP and TH negative (Figures 1A and 1B, top right). A group of 11 candidate transcription factors was selected based on their known functions in the development and survival of midbrain DA neurons (Table S1 available online), and was packaged into doxycycline (dox)-inducible lentiviruses and introduced into Pitx3-eGFP TTFs. Twelve days after infection, TH+ cells with neuronal morphology appeared in the cultures (Figure 1B, middle left and bottom panels) with eventually approximately 2% of the cells expressing *Pitx3* as indicated by eGFP staining (Figure 1C). We also reprogrammed wild-type TTFs as indicated by the appearance of DA neuron-like cells after viral transduction (Figure 1B, middle right). To determine which factors were critical

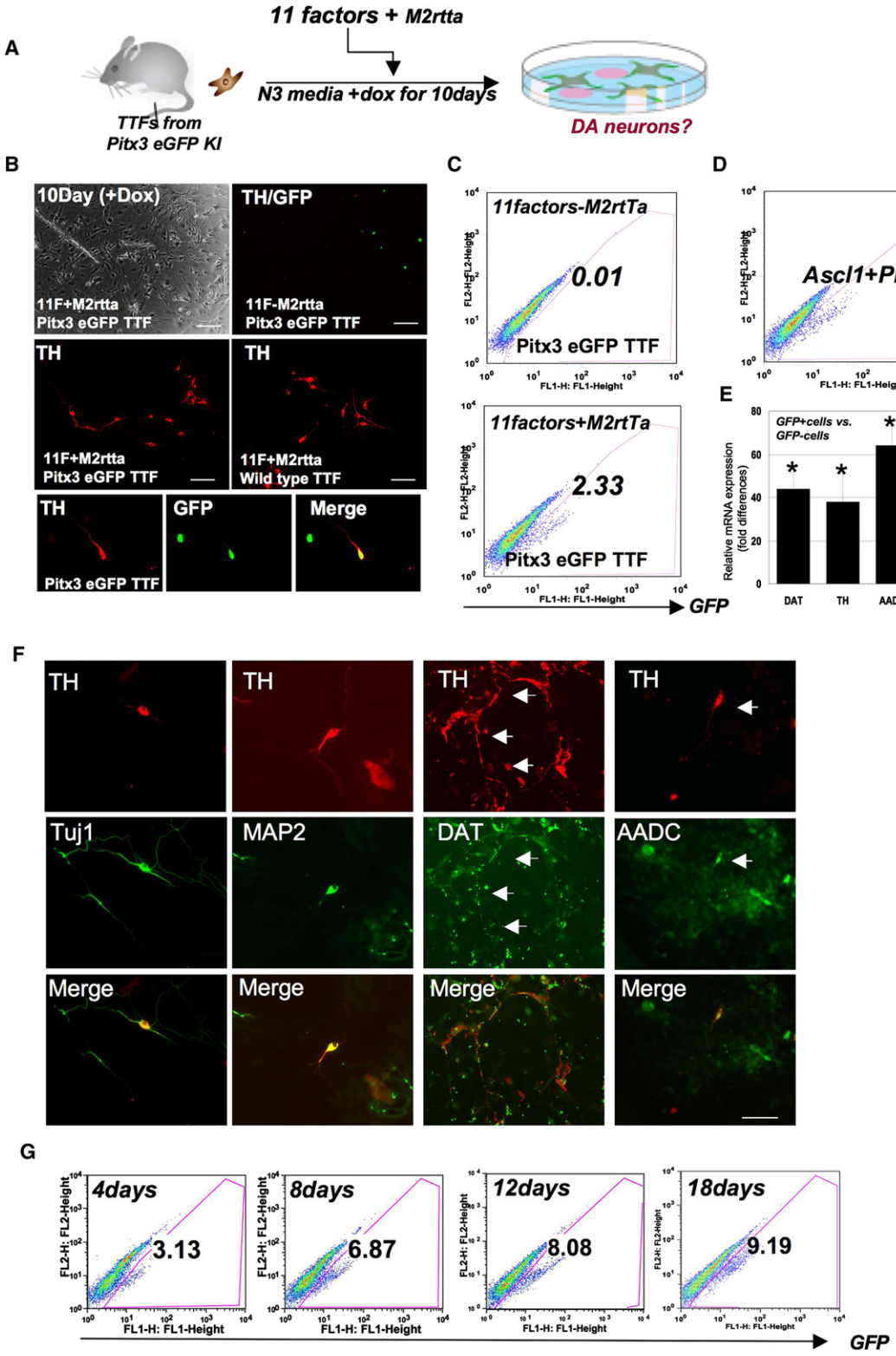

Figure 1. Direct Conversion of Fibroblasts into Functional DA Neurons

(A) Strategy for lineage reprogramming of iDA neurons from Pitx3-eGFP TTF. TTFs were transduced with lentiviral pools encoding 11 transcription factors, and cultured for 10 days in dox-containing N3 media.

(B) Morphology and immunofluorescence for TH+ DA neuron-like cells (red) in fibroblasts transduced with 11 transcription factors (top left panel). No TH+/GFP+ signal can be seen in control fibroblasts lacking M2rtTA (top right panel). TH+ DA neuron-like cells were detected in 11-factor-infected Pitx3-eGFP fibroblasts

for this process, we divided the 11 factors into three groups and tested the ability of different combinations of the pools to induce Pitx3-eGFP. Using this subtractive approach we found that a pool of eight factors lacking Pax6, Sox1, and Ngn2 generated Pitx3-eGFP+ cells more efficiently than the original pool of 11, whereas removal of the Acsl1, Myt1l, or Brn2 group or the Lmx1a, Lmx1b, Nurr1, Pitx3, or EN1 group failed to produce Pitx3-eGFP+ cells, suggesting that this combination of eight transcription factors was sufficient for the induction of Pitx3-eGFP+ cells (Figure S1E). To identify the key DA-inducing factors, we examined the effects of removing individual factors from the eight-factor pool. Surprisingly, eGFP+ cells were not detectable in TTF cultures infected with lentiviral pools lacking Ascl1, and pools lacking Pitx3 induced only a small number of eGFP+ cells (about 0.5%). However, pools lacking any of the remaining six factors were able to induce significant numbers of eGFP+ cells (Figure S1F). This result suggests that Ascl1 and Pitx3 are necessary for the induction of Pitx3-eGFP+ DA neurons. We also found that these two transcription factors alone were able to induce Pitx3-eGFP+ cells in 2%–3% of the target cells (Figure 1D). The expression of DA neuronal marker genes was determined using quantitative RT-PCR on FACS-purified Ascl1/Pitx3 transduced GFP+ and GFP− cells. The DA-neuron-specific markers examined included genes involved in the biosynthesis of dopamine [TH, aromatic L-amino acid decarboxylase (AADC)], dopamine storage [vesicular monoamine transporter 2 (VMAT2)], and dopamine uptake [dopamine transporter (DAT)], all of which were significantly upregulated in Pitx3-eGFP+ cells when compared to eGFP− cells (Figure 1E). However, the expression level of these genes was lower than that observed in primary Pitx3-eGFP+ DA neurons (Figure S1G) and we were not able to detect dopamine or electrophysiological activity (data not shown). We maintained the eGFP+ cell cultures for up to 4 weeks and did not observe significant maturation of DA neurons (data not shown). These results suggest that Pitx3-eGFP+ cells induced by Ascl1 and Pitx3 are not terminally differentiated DA neurons but may instead represent immature DA neurons. Several extrinsic and intrinsic factors that control maturation of DA neurons are functionally interconnected and cooperate to promote the terminal differentiation of DA neurons during neuronal development (Kim et al., 2002; Lee et al., 2000; Martinat et al., 2006). We therefore tested whether inclusion of additional factors could fully reprogram fibroblasts into functional DA neurons.

Several neurotrophic factors including Sonic hedgehog (Shh) and Fibroblast growth factor 8 (FGF8) appear to be critical for the specification and differentiation of developing midbrain DA neurons (Lee et al., 2000). To examine whether Shh and FGF8 promote DA neuron reprogramming, Ascl1 and Pitx3 transduced fibroblasts were cultured with Shh and FGF8 and the efficiency of iDA neuron generation was determined. Cultures treated with Shh and FGF8 generated about 5% Pitx3-eGFP+ cells, which is 2-fold more than in cultures treated with bFGF alone (Figure S1H). These data suggest that neurotrophic factors are critical components in promoting the generation of iDA neurons from fibroblasts. We also examined the DA-neuron-inducing activity of other genes by adding single factors to the Ascl1/Pitx3-infected cells. As shown in Figure S1I, the addition of Lmx1a, Nurr1, Foxa2, and EN1 in combination with Ascl1 and Pitx3 significantly enhanced the efficiency of eGFP+ induction, whereas overexpression of Sox1, Pax6, or Lmx1b had an inhibitory effect or no effect at all. Because of the positive effects of Lmx1a, Nurr1, Foxa2, and EN1 on the reprogramming process, we tested different combinations of these four factors along with Ascl1 and Pitx3 and found that the combination of all six factors (Ascl1, Pitx3, Lmx1a, Nurr1, Foxa2, and EN1) gave rise to the highest induction of eGFP+ cells 10 days after infection (Figure S1J). In addition, these six factors can induce the expression of DA neuronal marker genes more efficiently than any other combinations including the previously published three-factor combinations (Figure S1K), suggesting that the induced cells resemble midbrain DA neurons more closely than those generated using other factor combinations. Next, we examined reprogramming efficiency by flow cytometry on days 4, 8, 12, and 18 after viral transduction with six factors in combination with FGF8 and Shh. A significant number of eGFP+ cells were evident as early as day 4, reaching 8% by day 12 and a maximum of 9.1% of total cells by day 18 (Figure 1G). Additionally, Figure 1F shows that TH+ iDA neurons are positive for neuron-specific class III beta-tubulin (Tuj1) and microtubule-associated protein 2 (MAP2), both mature neuronal makers, and for DAT or AADC, which are markers of mature DA neurons. Furthermore, none of the TH+ cells coexpressed dopamine beta hydrolase (DBH), a marker for noradrenergic neurons. Other types of neurons including 5HT and motor neurons were also not detected in these cultures (data not shown).

We compared the gene expression profiles of two- and six-factor reprogrammed iDA neurons, fibroblasts, neural stem cells (NSCs), embryonic midbrain DA neurons, and adult midbrain DA neurons by quantitative RT-PCR (Figure 2A). While some variability in marker gene expression was seen, likely as a result of the inconsistent efficiency of viral infection, DA neuronal maker genes were significantly upregulated in six-factor-induced GFP+ cells and partially upregulated in two-factor-induced eGFP+ cells. We also observed induction of NSC markers, including Nestin, in two-factor-induced Pitx3-eGFP+ cells, but the expression of these genes was significantly lower in six-factor-induced Pitx3-eGFP+ cells. These results again suggest

(middle left panels), which are double-labeled with GFP (bottom panels). TH+ DA neuron-like cells (red) were detected from TTFs derived from wild-type mice (middle right panel). Scale bars = 100 μm.

(C) Flow cytometry analysis for induction of eGFP+ cells from Pitx3-eGFP TTFs transduced with 11 transcription factors (bottom panel). Control infection is also shown (top panel).

(D) Induction of eGFP+ cells from Pitx3-eGFP TTFs by the ectopic expression of only two factors, Ascl1 and Pitx3.

(E) Quantitative RT-PCR of the expression of DA-neuron marker genes on FACS-purified, Ascl1/Pitx3-induced eGFP+ and eGFP− cells. Ten days after infection, the expression of DA-neuron-specific genes was significantly upregulated in eGFP+ cells. Data represent mean ± SEM; three independent experiments were performed; ANOVA test, *$p < 0.05$.

(F) Immunostaining of iDA neurons for the mature neuronal and DA neuronal markers Tuj1, MAP2, DAT, and AADC. Scale bars = 100 μm.

(G) FACS analysis for eGFP induction from Pitx3-eGFP TTFs transduced with six reprogramming factors after 4, 8, 12, and 18 days.

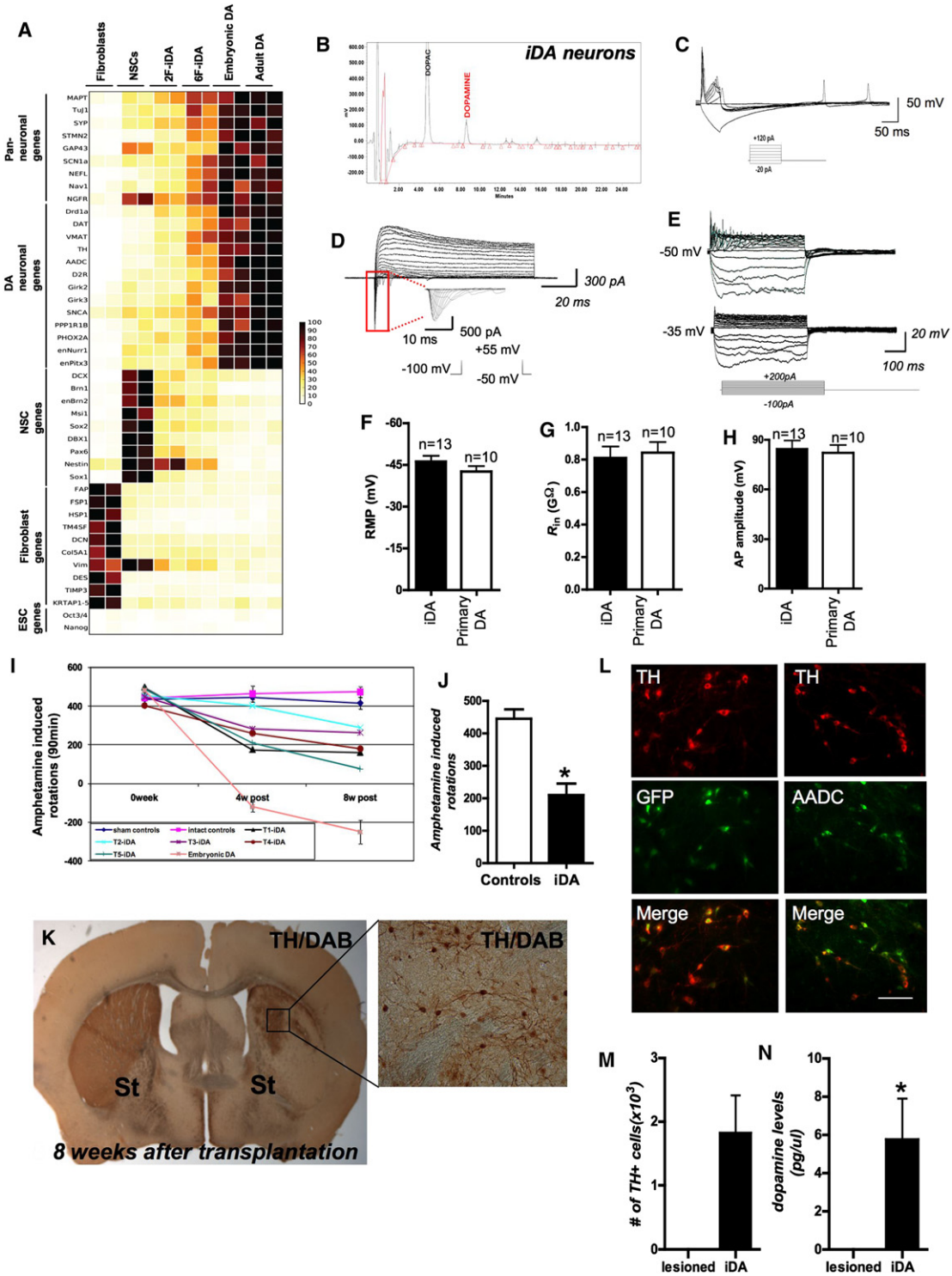

Figure 2. Functional Characterizations of iDA Neurons

(A) Gene expression profiling using quantitative RT-PCR analysis of neuronal, DA neuronal, ESC, and fibroblast marker gene expression in fibroblasts, NSCs, two- and six-factor-induced DA neurons, and primary embryonic and adult midbrain DA neurons. Rows represent the evaluated genes and heat map represents the relative expression of genes as indicated.

(B) Detection of dopamine from iDA neurons by RP-HPLC. The six-factor-infected cell cultures were analyzed 15 days after viral transduction and significant amounts of DA and the DA derivative 3,4 dihydroxyphenylactic acid (DOPAC) were detected in the six-factor-induced DA neurons.

(C–E) Electrophysiological properties of iDA neurons. (C) Representative recording of action potentials recorded from an iDA neuron. Bottom traces represent current injections (−20 pA to +120 pA), whereas top traces indicate voltage recordings. (D) Voltage-dependent membrane currents and depolarizing voltage

that two-factor-induced Pitx3-eGFP+ cells represent immature DA neurons and that additional factors are required for the maturation of two-factor-induced eGFP+ cells into differentiated DA neurons. Furthermore, we found a significant reduction of fibroblast marker gene expression in six-factor-induced eGFP+ cells to levels indistinguishable from those seen in primary Pitx3-eGFP+ cells. These results indicate that six-factor iDA neurons are similar at the molecular level to midbrain DA neurons. The dependence of iDA neurons on ectopic transgene expression was examined using a dox-inducible lentiviral system. We transduced Pitx3-eGFP TTFs with the dox-inducible factors along with M2rtTA and induced iDA neuron reprogramming with dox for 5 days. After eGFP expression was detected in the reprogramming cultures, dox was withdrawn and the cells were maintained for 7 days to allow complete silencing of exogenous gene expression (Figure S2A). We observed that Pitx3-eGFP expression was stably maintained in these cultures, demonstrating that the iDA neurons are phenotypically stable in the absence of ectopic factor expression (Figure S2B).

To test whether the reprogrammed cells have functional qualities of DA neurons, we examined dopamine production by reverse-phase high performance liquid chromatography (RP-HPLC). Significant levels of dopamine and the dopamine derivative 3,4 dihydroxyphenylactic acid (DOPAC) were detected in the iDA neurons (Figure 2B), in contrast to fibroblasts, which were negative for this derivative (Figure S2C). Importantly, we were able to detect dopamine release in the context of high potassium (56 mM)-induced depolarization in the iDA neurons (Figure S2D), as expected for functional neurons that produce and release dopamine. We also examined whether iDA neurons display electrophysiological properties characteristic of DA neurons. iDA neurons exhibiting a differentiated DA neuronal morphology were analyzed using whole-cell patch-clamp analysis and the identity of the analyzed cells was retrospectively confirmed by TH immunostaining. A current step protocol (−20 pA to +120 pA) elicited long-duration action potentials (>2 ms) in the majority of reprogrammed iDA neurons (13 out of 20 cells) (Figure 2C), in contrast to control fibroblasts, which were negative (Figure S2E). Fifteen days after dox treatment, the average resting membrane potential of iDA neurons was 48.23 ± 7.25 mV (mean ± SEM, n = 13), the input resistance was 1.13 ± 0.38 GΩ (mean ± SEM, n = 13), and action potential amplitude was 84.23 ± 18.69 mV (mean ± SEM, n = 13), providing evidence that the electrophysiological properties of the iDA neurons are similar to those of midbrain DA neurons (Figures 2F–2H). The iDA neurons also exhibited voltage-dependent ionic currents (Figure 2D). In addition, the action potentials evoked by depolarizing current injections in iDA neurons (top panel) were completely abolished by TTX administration (bottom panel) (Figure 2E), indicating the presence of well-developed Na channels in iDA neurons. Furthermore, in current-clamp mode we were able to inject prolonged hyperpolarizing current pulses (+20 pA to −140 pA) and observed that the voltage responses started to decline slowly in an iDA neuron (Figure S2F); this type of prominent time-dependent anomalous rectification is characteristic of the functional midbrain DA neurons (Rayport et al., 1992). In sum, these results indicate that the reprogrammed DA-producing neurons acquired functional properties that are highly similar to those of midbrain DA neurons.

Finally, we investigated whether iDA neurons can be effective in a rodent PD model for cell transplantation therapy. Pitx3-eGFP+ cells were FACS isolated from TTFs 12 days after transduction with six factors. The eGFP+ cells were implanted into the striatum of mice that had been lesioned with 6-hydroxydopamine (6OHDA) to mimic the DA loss that occurs in PD. Eight weeks after transplantation, the implanted Pitx3-eGFP+ cells led to a significant reduction in amphetamine-induced rotation scores in 6OHDA lesioned mice (Figures 2I and 2J) in contrast to sham transplanted or intact controls, which showed no rescue. The survival of the transplanted iDA neurons was assessed in sections stained for TH (Figure 2K). In control mice, complete loss of TH fibers in the striatum occurred 4 weeks after 6OHDA lesioning (Figure S2G), but mice transplanted with Pitx3-eGFP+ cells exhibited integrated grafts containing large numbers of DA neurons (350–1900 cells, Figure 2M). The grafted cells showed neuronal morphology and extended TH+ fibers into the deinnervated host striatum (Figure 2K). We confirmed that all transplanted eGFP+ cells expressed the DA neuron markers TH and AADC in vivo (Figure 2I), and elevated dopamine levels were detected in transplanted striatum (Figure 2N). These data

steps elicited fast inward sodium currents (bottom traces, magnified inset) and slow inactivating outward potassium currents (top traces). (E) Effect of tetrodotoxin (TTX) on action potential of iDA neurons. Top panel: iDA neuron before TTX application. Bottom panel: same neuron after treatment with TTX. Depolarizing current injections ranged from −100 pA to +200 pA in 10 mV steps. TTX completely inhibited the action potential evoked by depolarization current injections in iDA neurons.

(F–H) Quantification of membrane properties in iDA neurons at 15 days after infection. Numbers in the bars represent the numbers of recorded cells. Data are presented as mean ± SEM. RMP, resting membrane potentials; AP, action potential; Rin, membrane input resistances.

(I) Amphetamine-induced (4 mg/kg) rotational behaviors for 90 min in 6OHDA lesioned mice before the cell transplantation, and 4 and 8 weeks after the transplantation of Pitx3-eGFP+ cells (about 50,000 cells), control fibroblasts (sham controls), and primary embryonic midbrain Pitx3-eGFP+ cells into the lesioned striatum. Transplantation of reprogrammed Pitx3-eGFP+ cells and primary embryonic Pitx3-eGFP+ cells led to a significant reduction in amphetamine-induced rotation scores in 6OHDA lesioned mice 8 weeks after transplantation. None of the intact controls (6OHDA lesioned, but not recipients of cell transplants) or sham experiments (control fibroblasts) showed reduced rotation (n = 12). Data represent mean ± SEM; ANOVA test, *$p < 0.05$.

(J) Statistical analysis of amphetamine-induced rotational behaviors 8 weeks after transplantation. Data represent mean ± SEM; ANOVA test, *$p < 0.05$.

(K) Substantial graft-derived reinnervation of the lesioned striatum 8 weeks after transplantation. FACS-purified, Pitx3-eGFP+ cells were sorted and transplanted into the striatum of 6OHDA lesioned adult mice. The boxed area in (K) is shown at larger magnification to the left. Partial rescue of TH+ cells and fibers in 6OHDA lesioned striatum is shown, and most of the TH+ neurons show a large size and elongated shape typical of midbrain DA neurons.

(L) The grafted GFP+ cells coexpressed TH and another DA neuronal maker, AADC. Scale bars = 100 μm.

(M) Total TH+ cells in the graft (n = 5). Five brain slices with 50 μm thickness around the lesioned site were counted. Data represent mean ± SEM; ANOVA test, *$p < 0.05$.

(N) Summary of HPLC quantification of dopamine levels in both iDA neuron-transplanted and control striatum. Data represent mean ± SEM, (n = 5); ANOVA test, *$p < 0.05$.

indicate that transplanted iDA neurons are the major population of DA neurons after transplantation and demonstrate the functional capacity of the iDA neurons, suggesting that this type of strategy may potentially provide a useful therapeutic cell source for cell replacement therapy in PD.

In this study, we have demonstrated that the combined activity of Ascl1 and Pitx3 is sufficient to facilitate the conversion of fibroblasts into an immature DA neuronal cell fate, and that ectopic expression of additional transcription factors is required for maturation of two-factor-induced Pitx3-eGFP+ cells. Reprogramming to pluripotency is thought to involve numerous rounds of cell division, which appear to be critical for the completion of epigenetic changes associated with the acquisition of pluripotency (Hanna et al., 2009). In contrast, the reprogramming into functional neurons does not seem to require multiple cell divisions (Vierbuchen et al., 2010), and differentiated neurons are postmitotic. Thus, we hypothesized that induction of a functional DA neuron state might require the activity of additional factors. Consistent with this idea, we found that the addition of several other transcription factors to the original two-factor cocktail resulted in the upregulation of mature DA neuronal marker genes in Pitx3-eGFP+ cells. However, the expression levels of these DA genes did not reach the same level that is observed in primary Pitx3-GFP+ cells. Therefore, future studies need to be performed to identify additional DA-neuron-inductive factors, and possibly epigenetic modifiers, that can generate terminally differentiated iDA neurons indistinguishable from midbrain DA neurons. More importantly, we have shown the functional rescue of iDA neurons in 6OHDA lesioned PD animal models. Although amphetamine-induced rotational tests do provide a functional readout, this assay does not measure a clinical phenotype of PD. Thus, the ability of the iDA neurons to suppress Parkinson-like symptoms in other behavioral tests remains to be examined. Moreover, the number of cells with DA phenotype in the present grafts (350–1900) is considerably higher than the number estimated to be needed in grafts of mouse fetal DA neurons to compensate for amphetamine administration in 6OHDA lesioned mice (25–100 DA cells; Brundin et al., 1986). Thus, the functional efficacy of the mouse-fibroblast-derived iDA neurons described here appears to be relatively low, suggesting that the reprogramming procedure would need to be improved further to be of use in cell replacement strategies.

Our results have several implications for the potential use of iDA neurons for disease modeling and cell replacement therapy of PD. The generation of iDA neurons from abundant somatic cells such as fibroblasts in a short period of time makes this system attractive for autologous cell-based approaches. Furthermore, iDA neurons could provide a more homogenous cell source for modeling PD in vitro. Importantly, our approach avoids concerns surrounding the inherent tumorigenicity of ESCs or iPSCs when transplanted in an undifferentiated state. Therefore, the generation of iDA neurons could provide a reasonable cell source for pharmacological assays or cell replacement therapy for PD.

SUPPLEMENTAL INFORMATION

Supplemental Information for this article includes two figures, one table, and Supplemental Experimental Procedures and can be found with this article online at doi:10.1016/j.stem.2011.09.011.

ACKNOWLEDGMENTS

We are grateful to Dr. M. Li for the Pitx3-eGFP targeting construct. We thank Dr. M. Wernig, for kindly providing Ascl1, Brn2, and Mytl1 lentiviral constructs, and Dr. T. Petryshen for technical supports. We also thank R. Flannery for veterinary assistance, D. Fu for technical assistance, and B. Carey, D. Hockemeyer, Y. Li, G. Welstead, and C. Garrett-Engele for comments. This work was supported by grants from the National Institutes of Health (NIH R37 HD045022 (6-9)/RJ) and the Howard Hughes Medical Institute. R.J. is an adviser to Stemgent and a cofounder of Fate Therapeutics.

Received: August 12, 2011
Revised: September 7, 2011
Accepted: September 21, 2011
Published online: October 20, 2011

REFERENCES

Berke, J.D., and Hyman, S.E. (2000). Addiction, dopamine, and the molecular mechanisms of memory. Neuron *25*, 515–532.

Brundin, P., Nilsson, O.G., Strecker, R.E., Lindvall, O., Astedt, B., and Björklund, A. (1986). Behavioural effects of human fetal dopamine neurons grafted in a rat model of Parkinson's disease. Exp. Brain Res. *65*, 235–240.

Caiazzo, M., Dell'Anno, M.T., Dvoretskova, E., Lazarevic, D., Taverna, S., Leo, D., Sotnikova, T.D., Menegon, A., Roncaglia, P., Colciago, G., et al. (2011). Direct generation of functional dopaminergic neurons from mouse and human fibroblasts. Nature *476*, 224–227.

Eggan, K., Baldwin, K., Tackett, M., Osborne, J., Gogos, J., Chess, A., Axel, R., and Jaenisch, R. (2004). Mice cloned from olfactory sensory neurons. Nature *428*, 44–49.

Hanna, J., Saha, K., Pando, B., van Zon, J., Lengner, C.J., Creyghton, M.P., van Oudenaarden, A., and Jaenisch, R. (2009). Direct cell reprogramming is a stochastic process amenable to acceleration. Nature *462*, 595–601.

Hedlund, E., Pruszak, J., Ferree, A., Viñuela, A., Hong, S., Isacson, O., and Kim, K.-S. (2007). Selection of embryonic stem cell-derived enhanced green fluorescent protein-positive dopamine neurons using the tyrosine hydroxylase promoter is confounded by reporter gene expression in immature cell populations. Stem Cells *25*, 1126–1135.

Hedlund, E., Pruszak, J., Lardaro, T., Ludwig, W., Viñuela, A., Kim, K.-S., and Isacson, O. (2008). Embryonic stem cell-derived Pitx3-enhanced green fluorescent protein midbrain dopamine neurons survive enrichment by fluorescence-activated cell sorting and function in an animal model of Parkinson's disease. Stem Cells *26*, 1526–1536.

Huse, D.M., Schulman, K., Orsini, L., Castelli-Haley, J., Kennedy, S., and Lenhart, G. (2005). Burden of illness in Parkinson's disease. Mov. Disord. *20*, 1449–1454.

Ieda, M., Fu, J.-D., Delgado-Olguin, P., Vedantham, V., Hayashi, Y., Bruneau, B.G., and Srivastava, D. (2010). Direct reprogramming of fibroblasts into functional cardiomyocytes by defined factors. Cell *142*, 375–386.

Kim, J.-H., Auerbach, J.M., Rodríguez-Gómez, J.A., Velasco, I., Gavin, D., Lumelsky, N., Lee, S.-H., Nguyen, J., Sánchez-Pernaute, R., Bankiewicz, K., and McKay, R. (2002). Dopamine neurons derived from embryonic stem cells function in an animal model of Parkinson's disease. Nature *418*, 50–56.

Lee, S.-H., Lumelsky, N., Studer, L., Auerbach, J.M., and McKay, R.D. (2000). Efficient generation of midbrain and hindbrain neurons from mouse embryonic stem cells. Nat. Biotechnol. *18*, 675–679.

Martinat, C., Bacci, J.-J., Leete, T., Kim, J., Vanti, W.B., Newman, A.H., Cha, J.H., Gether, U., Wang, H., and Abeliovich, A. (2006). Cooperative transcription activation by Nurr1 and Pitx3 induces embryonic stem cell maturation to the midbrain dopamine neuron phenotype. Proc. Natl. Acad. Sci. USA *103*, 2874–2879.

Olanow, C.W., Kordower, J.H., and Freeman, T.B. (1996). Fetal nigral transplantation as a therapy for Parkinson's disease. Trends Neurosci. *19*, 102–109.

Pfisterer, U., Kirkeby, A., Torper, O., Wood, J., Nelander, J., Dufour, A., Björklund, A., Lindvall, O., Jakobsson, J., and Parmar, M. (2011). Direct

conversion of human fibroblasts to dopaminergic neurons. Proc. Natl. Acad. Sci. USA *108*, 10343–10348.

Rayport, S., Sulzer, D., Shi, W.X., Sawasdikosol, S., Monaco, J., Batson, D., and Rajendran, G. (1992). Identified postnatal mesolimbic dopamine neurons in culture: morphology and electrophysiology. J. Neurosci. *12*, 4264–4280.

Szabo, E., Rampalli, S., Risueño, R.M., Schnerch, A., Mitchell, R., Fiebig-Comyn, A., Levadoux-Martin, M., and Bhatia, M. (2010). Direct conversion of human fibroblasts to multilineage blood progenitors. Nature *468*, 521–526.

Vierbuchen, T., Ostermeier, A., Pang, Z.P., Kokubu, Y., Südhof, T.C., and Wernig, M. (2010). Direct conversion of fibroblasts to functional neurons by defined factors. Nature *463*, 1035–1041.

Wernig, M., Zhao, J.-P., Pruszak, J., Hedlund, E., Fu, D., Soldner, F., Broccoli, V., Constantine-Paton, M., Isacson, O., and Jaenisch, R. (2008). Neurons derived from reprogrammed fibroblasts functionally integrate into the fetal brain and improve symptoms of rats with Parkinson's disease. Proc. Natl. Acad. Sci. USA *105*, 5856–5861.

Wilmut, I., Schnieke, A.E., McWhir, J., Kind, A.J., and Campbell, K.H.S. (1997). Viable offspring derived from fetal and adult mammalian cells. Nature *385*, 810–813.

Zhao, S., Maxwell, S., Jimenez-Beristain, A., Vives, J., Kuehner, E., Zhao, J., O'Brien, C., de Felipe, C., Semina, E., and Li, M. (2004). Generation of embryonic stem cells and transgenic mice expressing green fluorescence protein in midbrain dopaminergic neurons. Eur. J. Neurosci. *19*, 1133–1140.

Zhou, Q., Brown, J., Kanarek, A., Rajagopal, J., and Melton, D.A. (2008). In vivo reprogramming of adult pancreatic exocrine cells to beta-cells. Nature *455*, 627–632.